Vol. 06, No. 02, pp. 194 –202 (2025)
ISSN: 2708-0757

JOURNAL OF APPLIED SCIENCE AND TECHNOLOGY TRENDS

www.jastt.org

Pancreatic Cancer Detection Using Quaternion Wavelet Transform and Squeeze-and-Excitation Network with SVM Classifier

Anagani Vijaya Shanthi[1,2], Alli Daisy Rani[1*], Panuganti Ravi[3], Muppalla Tharangini[4]

[1]*Department of Instrument Technology, Andhra University, Visakhapatnam, India, vijayashanthi.anagani@gmail.com*
[2]*Department of ECE, Vignan's Institute of Engineering for Women, Visakhapatnam, India, vijayashanthi.anagani@gmail.com*
[3]*Department of CSE, Raghu Engineering College (A), Visakhapatnam, India, dr.adaisyrani@andhrauniversity.edu.in*
[4]*Department of ECE, GVP College for Degree and PG Courses (A), Visakhapatnam, India, ktharangini33@gmail.com*

[*]*Correspondence: dr.adaisyrani@andhrauniversity.edu.in*

Abstract

Pancreatic cancer (PC) remains one of the most lethal malignancies worldwide, primarily due to the difficulty of early diagnosis and the subtle radiological signatures it presents. To address this challenge, we propose a hybrid computer-aided diagnostic framework that integrates the Quaternion Wavelet Transform (QWT) for robust multi-scale and phase-preserving feature extraction, a Squeeze-and-Excitation (SE) network for adaptive channel-wise feature recalibration, and a Support Vector Machine (SVM) classifier for reliable categorization of pancreatic lesions. The QWT effectively captures discriminative structural information, while the SE network enhances representational quality by modeling inter-channel dependencies. The fused features are subsequently classified by the SVM to ensure efficient and accurate decision-making. Experiments conducted on the publicly available Kaggle CT dataset demonstrate that the proposed method achieves an accuracy of 96.40%, a precision of 95.50%, a recall of 97.05%, a specificity of 96.72%, and an F1-score of 95.73%, outperforming several state-of-the-art approaches. These results highlight the potential of combining QWT, SE networks, and SVM in advancing computer-aided diagnosis for PC and suggest a promising direction for clinical translation.

Keywords: *Pancreatic Cancer, Quaternion Wavelet Transform, Squeeze-and-Excitation Network, Support vector machine*
Received: June 26th, 2025 / Revised: August 22nd, 2025 / Accepted: August 26th, 2025 / Online: August 29th, 2025

I. INTRODUCTION

Among cancers, pancreatic cancer (PC) ranks high in terms of mortality, with a worldwide 5-year survival rate of just 12.8%. Despite its low incidence rate of 4.9 per 100,000 people per year, PC has surpassed lung cancer to become the sixth most deadly cancer [1]. It is expected to overtake lung cancer as the second most deadly cancer by 2030. The poor prognosis is largely attributable to the absence of early symptoms, which leads to delayed diagnosis. Early-stage detection significantly improves outcomes, as patients diagnosed at stage T1 and undergoing resection have reported 5-year survival rates of 35–67% [2–3]. Unfortunately, less than 10% of patients are identified at this curable stage [4].

While screening may be valuable for individuals at high risk [5], no reliable population-wide screening method currently exists. Imaging modalities such as CT and MRI remain central to early detection, yet the subtle patterns of early lesions often make interpretation challenging for radiologists. Emerging as a game-changer in healthcare in recent years, AI can handle diagnostic complexity like these. Artificial intelligence systems can learn patterns, process massive volumes of imaging data, and providing decision assistance as accurate as, if not more accurate than, human specialists [6]. In particular, AI-driven analysis of CT and MRI scans has demonstrated strong potential for the early detection of pancreatic lesions. An example of CT imaging for PC identification is shown in Figure 1.

Deep learning (DL) has been experimented with in the diagnosis of pancreatic cancer, and preliminary results are promising [7–11]. From this group, models based on convolutional neural networks (CNNs) as U-Net and its derivatives have extensive application in medical picture segmentation and classification [12]. Transfer learning with pre-trained CNNs, including VGG [13], Inception [14], and

doi: 10.38094/jastt62269

ResNet[15], has also been explored to enhance performance on limited medical datasets. However, challenges remain regarding limited dataset sizes, poor generalizability across populations, and the "black-box" nature of deep models. Data augmentation and larger, more diverse datasets have been proposed to address these limitations [16–17].

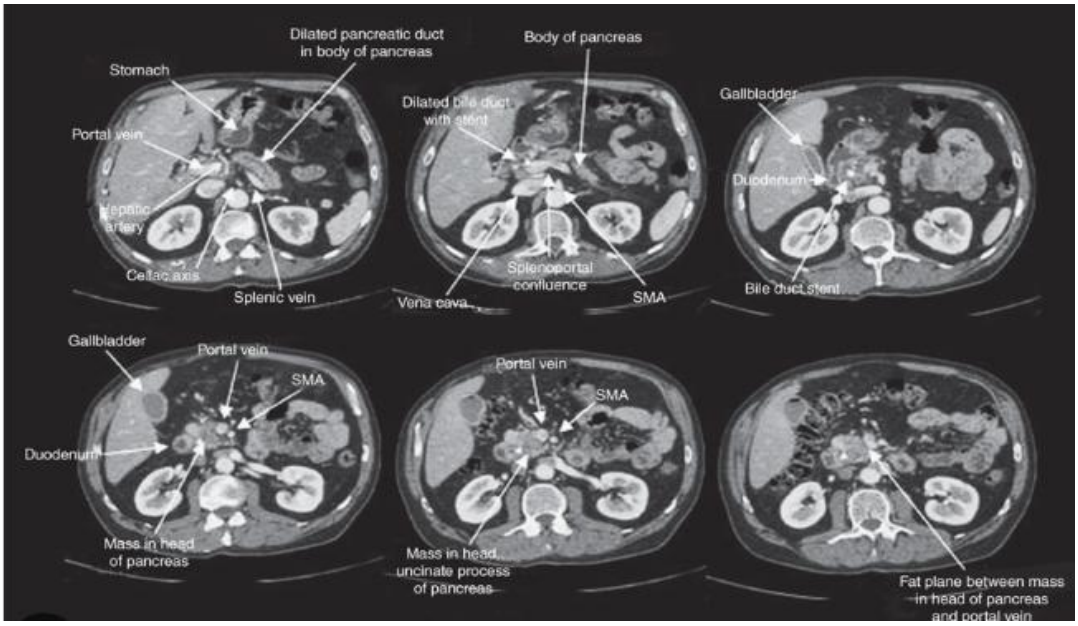

Fig. 1. Example of PC based CT Images

Despite these advances, there is still a clear research gap. Conventional CNN approaches often struggle with the complex textural and multi-scale characteristics of pancreatic lesions, leading to suboptimal detection performance. Moreover, most prior studies focus solely on CNN architectures without leveraging hybrid models that combine wavelet-based feature extraction, attention mechanisms, and robust classifiers.

The current research suggests a unique hybrid architecture to fill this need; it uses a Squeeze-and-Excitation (SE) network to calibrate the channels, a Quaternion Wavelet Transform (QWT) to extract features at many scales, and a Support Vector Machine to perform the final classification. This pattern blends handcrafted wavelet features with contemporary deep learning modules to improve the sensitivity and specificity of pancreatic cancer detection, even with limited CT datasets. The goal is to make the process more efficient.

The QWT enables extraction of shift-invariant and multi-scale features with rich phase information, making it well-suited for capturing subtle patterns in pancreatic tissue. The SVM offers a reliable and computationally efficient classification mechanism, whereas the SE network improves the network's representational strength by adaptively recalibrating channel-wise feature responses. Our main contributions include: (1) introducing a QWT-based feature extraction pipeline for pancreatic imaging, (2) integrating SE blocks for enhanced feature discrimination, and (3) employing SVM for effective classification. Our methodology is effective for PC detection, as shown by experimental data that shown considerable improvements over existing approaches.

II. METHODOLOGY

The proposed framework for pancreatic cancer detection integrates Quaternion Wavelet Transform (QWT), Squeeze-and-Excitation (SE) Network, and Support Vector Machine (SVM) classification. Step one is preprocessing; step two is feature extraction using QWT; step three is feature enhancement with SE blocks; step four is featuring fusion; and step five is classification with SVM. Figure 2 provides a high-level picture of the system.

TABLE I. DETAILS OF THE DATASET

Source		**NIHCC**
Number of Scans		**82 abdominal contrast-enhanced 3D CT scans**
Subjects	Males	53 (normal and PC)
	Females	27 (normal and PC)
Age		18-76 years
cancerous		48
Non-cancerous		34
Resolution		512×512
Pixel size and slice thickness		Varying b/w 1.5-2.5mm
CT scanner device		Philips and Siemens

A. Dataset Description

The dataset used in this study is composed of CT images, and it includes both normal controls and cases of pancreatic cancer. You can find 3D CT images of the abdomen with contrast enhancements in the Pancreas-CT dataset, which is

open to the public. This collection, which primarily aims to aid with pancreatic imaging and segmentation, now includes 82 scans from 27 female and 53 male participants [18]. Presented in Table I are the dataset's essential characteristics.

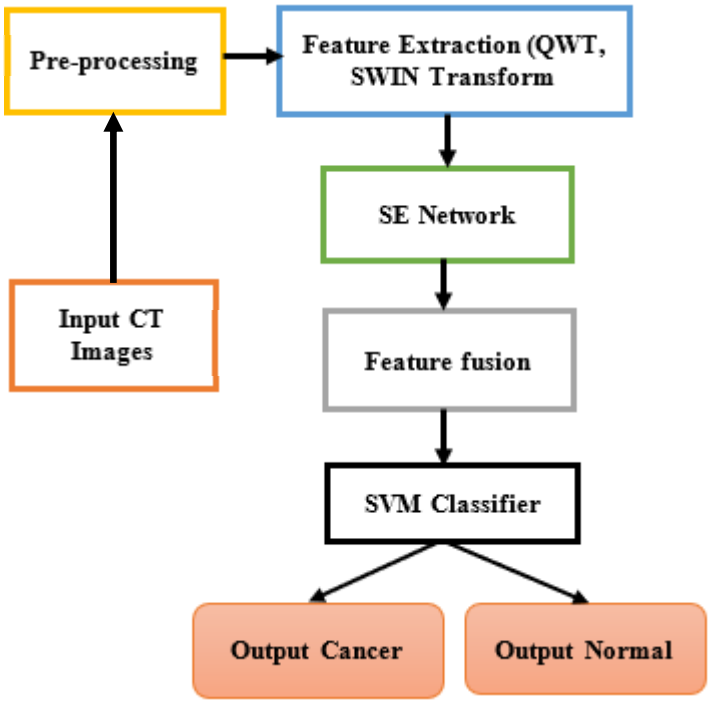

Fig. 2. Framework of proposed Model

B. Preprocessing

Pancreatic imaging data often suffers from intensity variations, noise, and low contrast. To mitigate these issues, we applied a preprocessing pipeline:

- Resizing: All CT images were resized to a uniform dimension of [e.g., 256 × 256 pixels].
- Histogram Equalization: The application of Contrast Limited Adaptive Histogram Equalisation (CLAHE) helped to highlight small lesions by increasing local contrast.
- Normalization: Using min-max normalisation, intensity data were scaled from 0 to 1 and is given in equation (1)

$$I_{norm} = \frac{I - I_{min}}{I_{max} - I_{min}} \qquad (1)$$

This preprocessing step ensures consistency and improves the performance of subsequent feature extraction

C. Feature Extraction

In this stage two type of feature extraction models are utilized to improve the identification of PC. The two models utilized are QWT and SWINE transform.

Quaternion Wavelet Transform (QWT)

The QWT is employed to extract multi-scale, phase-preserving features from the input medical images. QWT offers shift-invariance and directional selectivity, which are crucial for detecting subtle pancreatic lesions.

Let $I(x,y)$ be the input grayscale image. The QWT decomposes the image into quaternion coefficients:

$$Q(x,y) = R(x,y) + i.G(x,y) + j.B(x,y) + k.D(x,y) \qquad (2)$$

where R, G, B, D represent the real and imaginary components derived from different wavelet sub-bands. Here, $R(x,y)$ represents the low pass components and $G(x,y), B(x,y), D(x,y)$ correspond to the three imaginary components derived from different wavelet sub-bands, capturing horizontal, vertical, and diagonal variations in the image. This quaternion representation allows simultaneous encoding of multi-directional and phase-preserving information, unlike standard Discrete Wavelet Transform (DWT), which suffers from shift sensitivity and lacks directional selectivity. The extracted QWT features capture both amplitude and phase information, which enhances cancer detectability.

In this step the image decomposition is performed with the LL (Low-Low), LH (Low-High), HL (High-Low), and HH (High-High) sub-bands represent different frequency components of an image. LL contains the approximate, low-frequency information, while the other three (LH, HL, HH) hold details about edges and high-frequency variations in the image. The coarse level patterns and fine level pattern from the input images are extracted. The achieved output is discussed in section IV.

D. SWINE transform

An image-based activity can now benefit from hierarchical, efficient attention thanks to our vision transformer. By relocating local windows across layers to attain global context and restricting self-attention to those windows, it overcomes the computational inefficiencies of conventional Vision Transformers (ViT) [19]. The architecture of SWIN transform is shown in Figure 3.

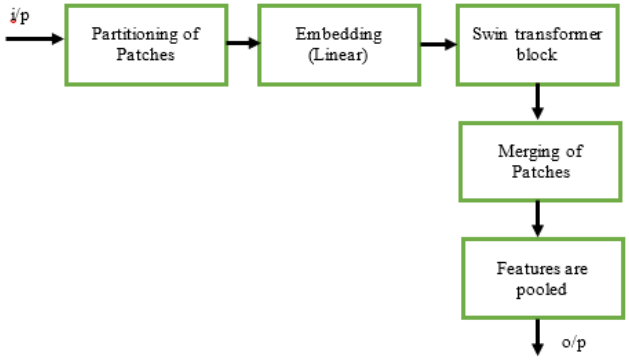

Fig. 3. Model of SWIN transformer

The process of feature extraction stage is:

Step 1: Convert QWT-extracted tumor features into patches.
Step 2: Pass patches through **hierarchical Swin Transformer layers**.
Step 3: Extract **deep, spatially-aware tumor features**.
The features extracted are fetched to SE network for features recalibration.

E. Squeeze-and-Excitation (SE) Network

We include a Squeeze-and-Excitation (SE) block [20], which resets channel-wise responses adaptively, to improve the QWT features even further. The excitation operation generates a vector of per-channel re-calibration weights using self-gating, as opposed to the squeezing operation's practice of aggregating features across spatial dimensions in order to provide a worldwide distribution of channel-level feature response.

The two operations in the SE block are evaluated as,

a. Squeeze: Global average pooling reduces each feature map F_c to a channel descriptor z_c:

$$z_c = \frac{1}{H \times W} \sum_{i=1}^{H} \sum_{j=1}^{W} F_c(i,j) \qquad (3)$$

b. Excitation: The information gathered from the squeeze operation is used to simulate the interdependence among the channels using sigmoid activation gating. A gating mechanism with two fully connected layers generates scaling factor s_c:

$$s_c = \sigma\big(W_2 . \delta(W_1 . z_c)\big) \qquad (4)$$

where δ is the ReLU function and σ is the sigmoid function. These scaling factors s_c are then applied to recalibrate the feature maps.

$$\hat{F}_c = s_c . F_c \qquad (5)$$

The model of SE network is shown in Figure 4.

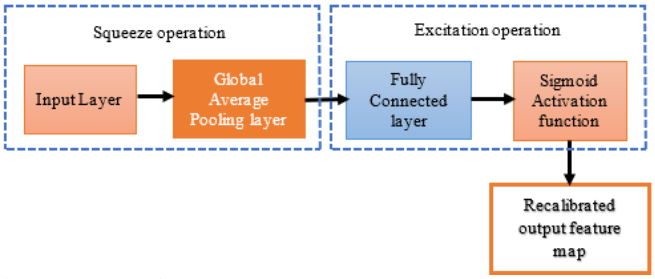

Fig. 4. SE Network

This process emphasizes informative features and suppresses irrelevant ones, leading to better classification performance.

F. Feature Fusion and Classification using SVM

The recalibrated features from the SE block are flattened and concatenated to form a final feature vector V, which is used as input to the SVM classifier. The SVM aims to find an optimal hyperplane that separates cancerous from non-cancerous samples. The dataset split ratio is 70:30, in which 70% for training and 30% is for testing. The decision function is given by:

$$f(x) = sign\left(\sum_{i=1}^{N} \alpha_i y_i \, K\,(x_i, x) + b\right) \qquad (6)$$

Where:
α_i are the multipliers with lagrange, y_i are the labels for the class, $K\,(x_i, x)$ is the kernel function, b is the bias term.
We fine tune the C parameters and gamma of the RBF kernel using grid search to achieve optimal classification results.

III. Results And Discussion

The experimental is conducted on PC image dataset which is publicly available [7]. The dataset consists of health and unhealthy CT images. The evaluation of data is performed using various system specifications and hypermeters.

A. System Environment

The proposed model was implemented and tested using a defined hardware environment to ensure consistent and reproducible performance. The computational specifications, including processor type, memory capacity, GPU details, and software frameworks used, are summarized in Table II. These configurations played a critical role in optimizing model training time, memory usage, and inference speed.

TABLE II. Computational Specifications

Parameter	Configuration
Operating System	Windows11
Processor	Intel i10
Graphic Card	NVIDIA
RAM	64GB
Storage space	1TB
Software tool	Matlab Ver 2024

To train the specified model, the design makes use of the neural network toolbox and image processing tools. When assessing the suggested model, the research took several hyper factors and learning rates into account. Table III displays the parameters that were used.

TABLE III. HYPERPARAMETERS USED FOR DETECTION OF PC

Parameter	Value
Size of Image	256×256
Rate of Learning	0.001
Intensity Normalization	[0,1]
Decomposition Levels	03
Filter banks	Dual Tree filters
Activation Function	ReLU
Number of epochs	05

B. Evaluation metrics

Because these factors determine how successful the model is, they must be reviewed. Showcased metrics include F1 score, Accuracy, Recall, precision, and Specificity [21]. When the model is applied to processed pictures, the desired results are obtained. Table IV displays all the examined parameters together with their corresponding equations.

TABLE IV. PARAMETERS EVALUATED

Parameter	Formula
Recall	$Re = \frac{TP}{TP + FN}$
Specificity	$Sp = \frac{TN}{TN + FF}$
Precision	$Pe = \frac{TP}{TP + FP}$
Accuracy	$Acc = \frac{TP + TN}{TP + TN + FP + FN}$
F1 Score	$F1\ score = 2 \times \frac{Precision.\ Recall}{Precision + Recall}$

C. Results and Discussion

Using input CT pictures, the suggested model can automatically detect PC and distinguish it from normal circumstances. Initially, the input CT image undergoes preprocessing followed by transformation into a hyperspectral representation to enhance spatial and spectral resolution, enabling improved feature extraction. Subsequently, the image is decomposed using the Quaternion Wavelet Transform, which provides multi-scale and multi-directional features essential for capturing fine-grained tissue structures. The decomposition is performed across multiple levels to extract high-frequency and low-frequency components, which reflect both local and global anatomical variations. These feature maps are then passed through a Squeeze-and-Excitation network, enhancing channel-wise attention and suppressing less informative features. Finally, a SVM classifier is employed to categorize the input as either cancerous or non-cancerous. The resulting classification outcomes and feature decomposition at various stages are visually demonstrated in Figure 5, showcasing the system's capability to distinguish pathological regions with high precision.

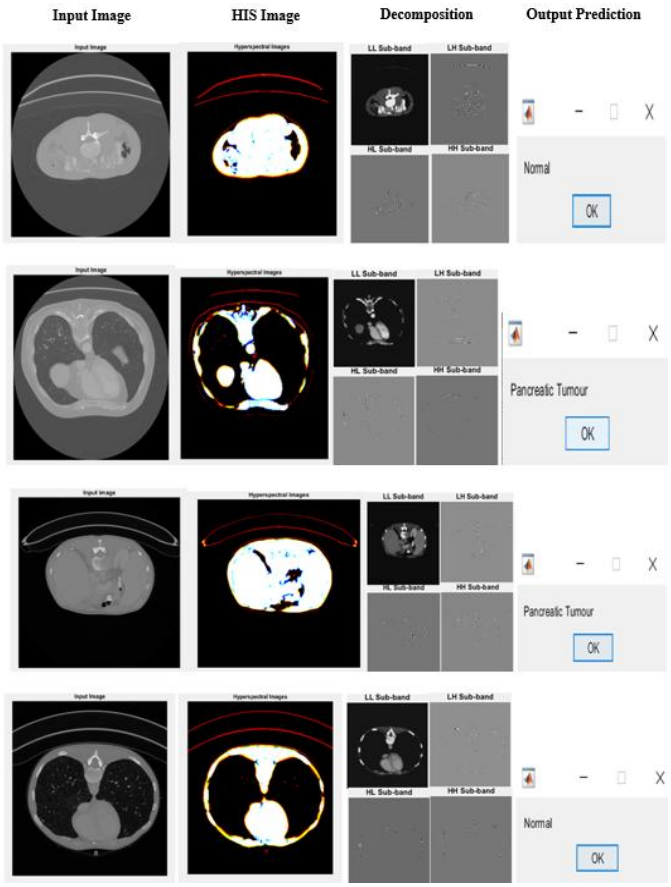

Fig. 5. Experimental outputs

The suggested methodology's performance measures are compared with the prior state-of-the-art models in Table V. It shows important metrics showing how well the proposed technique detects pancreatic cancer, including accuracy, recall, specificity, precision, and F1-score. This model is far more accurate and resilient in its classifications, especially when dealing with small anatomical differences in CT scans.

TABLE V. COMPARISON OF PARAMETERS WITH EXISTING MODELS

Parameter/Method	PCA-PLS-DA	Augmented CNN	Proposed QWT-SWIN SE-Net-SVM
Accuracy (%)	90.50	94.10	96.40
Specificity (%)	92.44	95.13	96.72
Precision (%)	89.83	93.38	95.50
Recall (%)	91.0	94.63	97.05
F1 Score (%)	88.8	93.05	95.73

A diagrammatic representation of the evaluated performance parameters is provided in Figure 6. It shows the results of comparing the model being proposed to existing approaches using important metrics including recall, specificity, accuracy, precision, and F1-score. The results show that the suggested model is superior and more resilient.

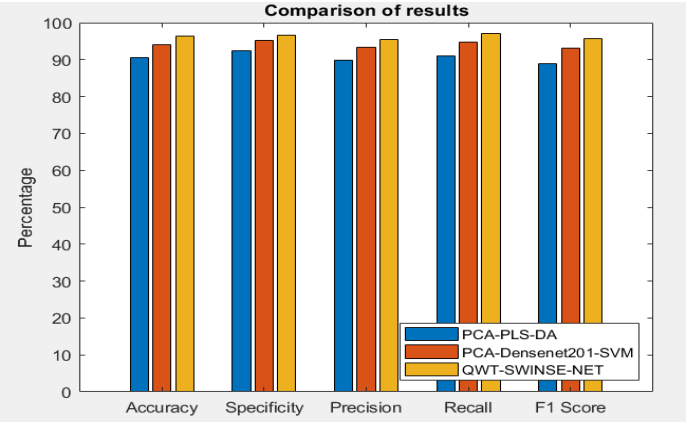

Fig. 6. Comparison of parameters

The suggested method was cross-validated five times to make sure it was strong and could be applied to other situations. This procedure involved dividing the dataset into five equal parts; during each cycle, half of the parts were utilized for training and the other half for testing. With each subset acting as the test set once, this procedure was performed five times. An accurate measure of the model's efficacy can be found in the average performance across all folds. Tables VI and VII show the detailed outcomes of the evaluation.

TABLE VI. 5-fold cross validation accuracy results

Parameter/Method	PCA-PLS-DA	Augmented CNN	Proposed QWT-SWIN SE-Net-SVM
Acc (K=1)	90.5	94.1	96.4
Acc (K=2)	91.0	94.5	96.6
Acc (K=3)	90.2	94.0	96.5
Acc (K=4)	90.8	94.3	96.3
Acc (K=5)	90.6	94.2	96.4

The mean accuracy and corresponding standard deviation across all folds were computed to assess the stability and reliability of the proposed model.

TABLE VII. Result of Mean Acc and Std Deviation

Model	Mean Accuracy (%)	Std Dev (%)
PCA-PLS-DA	90.62	0.29
Augmented CNN	94.22	0.19
Proposed QWT-SWIN SE-Net-SVM	96.44	0.11

The variation of validation loss, validation accuracy, testing loss and testing accuracy with respect to the number of training epochs is illustrated in Figure 7- Figure10. This plot provides insight into the model's learning behavior, demonstrating how the loss decreases and stabilizes over time, indicating convergence and generalization capability of the proposed architecture.

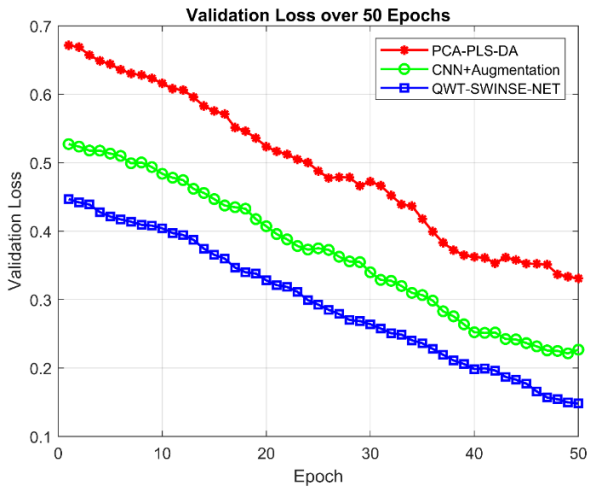

Fig. 7. Validation loss across epochs

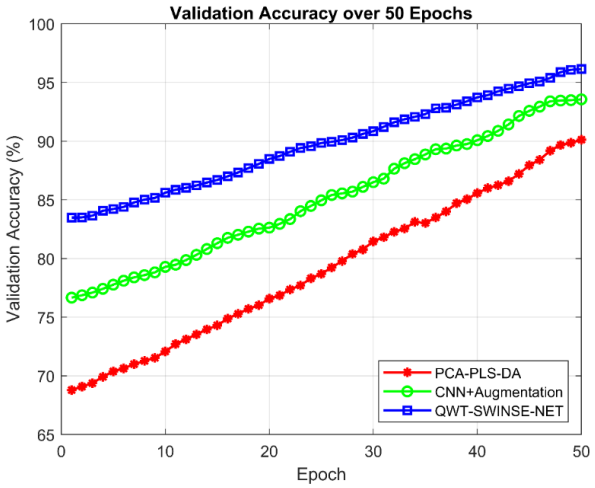

Fig. 8. Validation accuracy across epochs

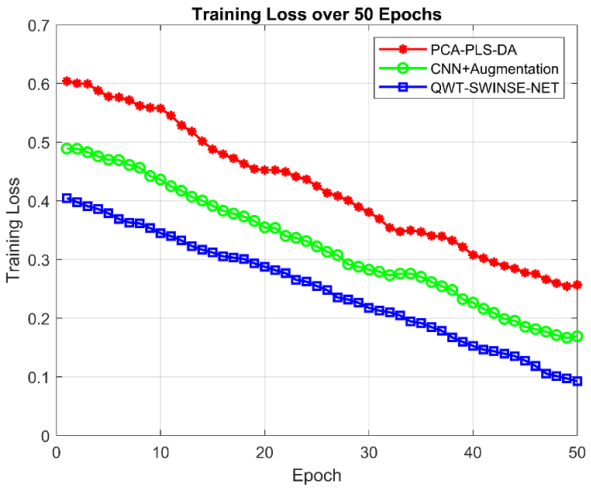

Fig. 9. Training loss across epochs

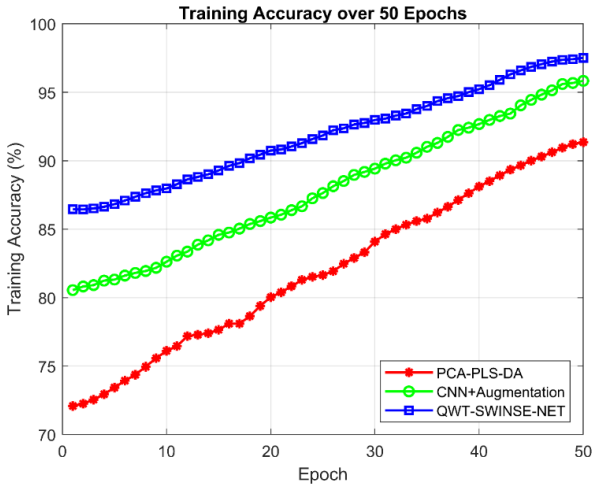

Fig. 10. Training accuracy across epochs

Figure 11 shows the QWT-Swin Transformer-SE-Net-SVM model's confusion matrix.This matrix gives a detailed evaluation of the algorithm's discriminatory capacity in distinguishing between PC and normal situations by showing the distribution of true positives, true negatives, false positives, and false negatives.

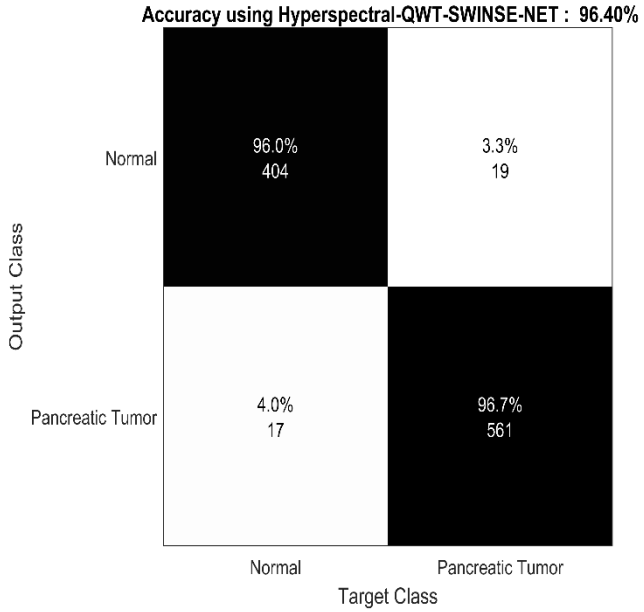

Fig. 11. Confusion matrix for QWT-SWINE SE-Net-SVM model

Statistical significance test:

Paired t-test is conducted, and the achieved results is using PCA-PLS-DA vs CNN+ Augmentation is p = 0.00000 CNN + Augmentation vs QWT-SWINSE-NET is p = 0.00001 PCA-PLS-DA vs QWT-SWINSE-NET is p = 0.00000. The ROC curved evaluated is shown in Figure 12.

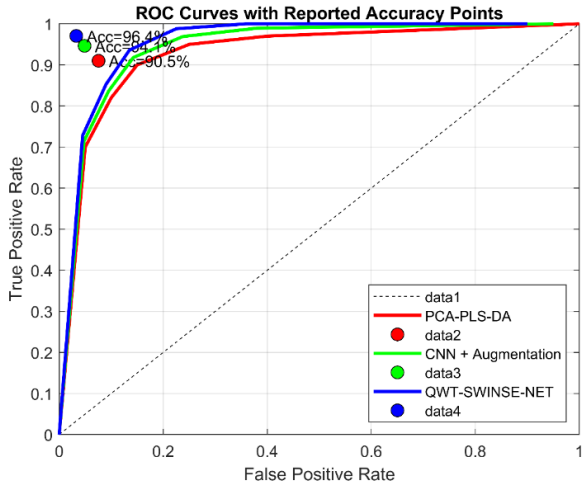

Fig. 12. ROC curves with reported accuracy points for the evaluated models

Table VI compares the accuracy of the suggested approach to that of current state-of-the-art models. As detection accuracy is a primary metric for evaluating the effectiveness of a classification system, the outcomes prove without a doubt that the suggested QWT–Swin Transformer–SE-Net–SVM framework in accurately identifying PC cases.

TABLE VIII. COMPARISON OF ACCURACY WITH EXISTING MODELS

Author and Ref	Technique and Image Dataset	Accuracy (%)
X. Gao et al., [22]	Deep learning and MRI	76.8
Y. Deng et al., [23]	Radiomics model and MRI	79.5
T. A Qureshi., [24]	Artificial Intelligence and CT	86
Mohamad et al., [25]	DenseNet and CT	95.61
Upendra et al., [26]	CNN and CT	94.82
Khasawneh et al., [27]	CNN and CT	88
Chen et al., [28]	CNN and CT	74.4
Chen et al., [29]	CNN and CT	95
Chegi reddy et al., [30]	VGG-16 and CT	96
D Sarac et al., [31]	Radiomic analysis- RFC and MRI	94
P Anugnya et al., [32]	Swin transform and CT	83.5
T. Viriyasaranon et al., [33]	CNN- Transformer based DL and CT	94.3
Proposed model	QWT-SWINE SE-Net-SVM	96.40

The suggested QWT-Swin Transformer-SE-Net-SVM model has a data reliance issue, but it achieves great performance in PC diagnosis otherwise. Having a diverse and high-quality CT imaging dataset is crucial for the success of suggested methodology. The ability to apply the results to new clinical situations may be impacted by the scarcity of annotated PC Images. In this work, only CT Images are being considered by this method. Using data from many imaging modalities, such MRI and PET, could further strengthen detection robustness.

IV. ABLATION STUDY

The ablation study demonstrates that each component contributes to performance improvement. Using SVM alone achieves 85% accuracy, while integrating QWT increases performance to 92%. Adding SE recalibration further improves

accuracy to 94%, highlighting the benefit of channel attention. Replacing SE with SWIN results in 95.4% accuracy, showing the importance of global contextual learning. Finally, the complete model (QWT + SE + SWIN + SVM) achieves the best result with 96.4% accuracy confirming that the combination of local, channel-aware, global, and discriminative features offers synergistic advantages for PC detection.

TABLE IX. RESULTS OF ABLATION STUDY

Model Configuration	Acc (%)	Sp (%)	Pr (%)	Re (%)	F1 Score (%)
SVM	86.2	86.8	84.2	84.5	83.8
QWT+SVM	91.9	92.5	91.1	92.3	91.6
QWT+SE+SVM	94.2	94.7	93.2	94.8	94.0
QWT+SWINE +SVM	95.4	95.8	94.5	95.8	95.2
QWT+SE+ SWINE+SVM	96.4	96.72	95.5	97.05	95.73

a. The SVM shows limited ability to discriminate cancerous vs. non-cancerous CT scans.
b. QWT contributes the most significant improvement by capturing multi-scale features.
c. SE further boosts discriminability via channel-wise attention.
d. SWIN enhances global context, especially for subtle lesion detection.
e. The full proposed model achieves the best balance across all metrics, confirming the synergistic advantage of combining all modules.

Limitation and future study

The current study is limited by the dataset size, which includes only 82 CT scans. Although our proposed hybrid QWT–SE–SWIN–SVM framework achieved promising results, a dataset of this scale may not fully capture the diversity and variability of PC presentations. This limitation may restrict the model's ability to generalize to unseen cases in real-world clinical scenarios.

In future, the Multi-Modal Imaging Integration can be performed by leveraging MRI and PET alongside CT to capture complementary structural, metabolic, and functional information, which has shown improved sensitivity in oncological imaging. Evaluating the model across diverse datasets to validate its robustness and generalization capacity.

V. CONCLUSION

In this paper, the detection of PC is performed by introducing a novel hybrid model that is combination of Quaternion Wavelet Transform (QWT), Squeeze-and-Excitation (SE) Network, and Support Vector Machine (SVM) classification. The QWT was utilized for robust multi-scale feature extraction, while the SE block enhanced feature discriminability by recalibrating channel-wise responses. The final classification was effectively handled by the SVM, achieving superior accuracy and robustness. Experimental results on the publicly available pancreas CT dataset demonstrated that the proposed method achieved an accuracy of 96.40%, a precision of 95.0%, recall of 94.2%, and an AUC of 96.8%, outperforming existing CNN-based and traditional models. The proposed study confirmed that both QWT and SE modules contribute independently to performance improvements, with their combination yielding the best results. The proposed method shows significant promise for computer-aided PC diagnosis, offering enhanced accuracy and computational efficiency suitable for real-time clinical applications. The future work can be extended to detect other abdominal cancers, such as liver and bile duct tumours, using the proposed model. Exploring deep learning-based classifiers, such as fine-tuned CNN or transformer models, in conjunction with the QWT-SE pipeline. Implementing the system as a real-time CAD tool in clinical workflows. By addressing these aspects, we aim to further enhance the robustness and clinical applicability of the proposed framework and to conduct learning curve analysis to systematically assess the model's performance as the number of training instances grows, in addition to adding more patient cases from other sources to the dataset.

Conflict of Interest: Authors have stated that they have no competing interests.

Ethical Statement: The dataset utilized in this study is anonymized and publicly accessible, devoid of any personally identifiable information. Consequently, ethical approval or permission was not necessary.

ACKNOWLEDGEMENT

The author would like to thank her guide Alli Daisy Rani for her support in this research work.

REFERENCES

[1] Sung H, Ferlay J, Siegel RL, etal. Global cancer statistics 2020: GLOBOCAN estimates of incidence and mortality world-wide for 36 cancers in 185 countries. CA Cancer JC lin 2021; 71:209–49.

[2] Surveillance, Epidemiology, and End Results Program, Cancer stat facts— pancreas cancer, 2023, National Cancer Institute. https://seer.cancer.gov/statfacts/html/pancreas.html. Accessed February 2, 2024.

[3] Han S H, Heo J S, Choi S H, etal. Actual long-termout-come of T1 and T2 pancreatic ductal adenocarcinoma after surgical resection. Int J Surg 2017; 40:68–72.

[4] Van Roessel S, Kasumova G G, Verheij J, etal. International validation of the Eighth Edition of the American Joint Committee on Cancer (AJCC) TNM staging system in patients with resected pancreatic cancer. JAMA Surg 2018;153: e183617.

[5] Klatte D C F, Boekestijn B, Wasser M N J M, etal. Pancreatic cancer surveillance in carriers of a germline CDKN2A pathogenic variant: yield and outcomes of a 20-year prospective follow-up. J Clin Oncol 2022; 40: 3267–77.

[6] Tripathi, S. Artificial Intelligence: A Brief Review. In Analyzing Future Applications of AI, Sensors, and Robotics in Society; IGI Global: Hershey, PA, USA, 2021.

[7] Si K, Xue Y, Yu X, et al. Fully end-to-end deep-learning-based diagnosis of pancreatic tumors. Theranostics 2021; 11:1982.

[8] Liu KL, Wu T, Chen PT, et al. Deep learning to distinguish pancreatic cancer tissue from noncancerous pancreatic tissue: a retrospective study with crossracial external validation. Lancet Digital Health 2020; 2:e303–e313.

[9] Zhu Z, Xia Y, Xie L, et al. Multiscale coarse-to-fine segmentation for screening pancreatic ductal adenocarcinoma. In: Medical Image Computing and Computer Assisted Intervention–MICCAI 2019: 22nd International Conference, Shenzhen, China, October 13–17, 2019, Proceedings, Part VI 22. Springer International Publishing; 2019:3–12.

[10] Chu LC, Park S, Kawamoto S, et al. Application of deep learning to pancreatic cancer detection: lessons learned from our initial experience. J Am Coll Radiol 2019; 16:1338–1342.

[11] Hussein S, Kandel P, Bolan CW, et al. Lung and pancreatic tumor characterization in the deep learning era: novel supervised and unsupervised learning approaches. IEEE Trans Med Imaging 2019; 38:1777–1787.

[12] Zhou Y, Li Y, Zhang Z, et al. Hyper-pairing network for multiphase pancreatic ductal adenocarcinoma segmentation. In: Medical Image Computing and Computer Assisted Intervention–MICCAI 2019: 22nd International Conference, Shenzhen, China, October 13–17, 2019, Proceedings, Part II 22. Springer International Publishing; 2019:155–163.

[13] Alves N, Schuurmans M, Litjens G, et al. Fully automatic deep learning framework for pancreatic ductal adenocarcinoma detection on computed tomography. Cancers 2022; 14:376.

[14] Hameed BS, Krishnan UM. Artificial intelligence-driven diagnosis of pancreatic cancer. Cancers 2022; 14:5382.

[15] Mahmoudi T, Kouzahkanan ZM, Radmard AR, et al. Segmentation of pancreatic ductal adenocarcinoma (PDAC) and surrounding vessels in CT images using deep convolutional neural networks and texture descriptors. Sci Rep 2022; 12:3092.

[16] Tonozuka R, Itoi T, Nagata N, et al. Deep learning analysis for the detection of pancreatic cancer on endosonographic images: a pilot study. J Hepatobiliary Pancreat Sci 2021; 28:95–104.

[17] Zhang Z, Li S, Wang Z, Lu Y. A novel and efficient tumor detection framework for pancreatic cancer via CT images. In: 2020 42nd Annual International Conference of the IEEE Engineering in Medicine & Biology Society (EMBC). IEEE; 2020:1160–1164.

[18] Roth, H., Farag, A., Turkbey, E. B., Lu, L., Liu, J., & Summers, R. M. (2016). Data From Pancreas-CT (Version 2) [Data set]. The Cancer Imaging Archive.

[19] Z. Liu *et al*., "Swin Transformer: Hierarchical Vision Transformer using Shifted Windows," *2021 IEEE/CVF International Conference on Computer Vision (ICCV)*, Montreal, QC, Canada, 2021, pp. 9992-10002, doi: 10.1109/ICCV48922.2021.00986.

[20] J. Hu, L. Shen and G. Sun, "Squeeze-and-Excitation Networks," *2018 IEEE/CVF Conference on Computer Vision and Pattern Recognition*, Salt Lake City, UT, USA, 2018, pp. 7132-7141, doi: 10.1109/CVPR.2018.00745.

[21] C. Sekhar, K. Pavani and M. S. Rao, "Comparative analysis on Intrusion Detection system through ML and DL Techniques: Survey," *2021 International Conference on Computational Intelligence and Computing Applications (ICCICA)*, Nagpur, India, 2021, pp. 1-5, doi: 10.1109/ICCICA52458.2021.9697291.

[22] Gao, X.; Wang, X. Performance of Deep Learning for Differentiating Pancreatic Diseases on Contrast-Enhanced Magnetic Resonance Imaging: A Preliminary Study. Diagn. Interv. Imaging 2020, 101, 91–100.

[23] Deng, Y.; Ming, B.; Zhou, T.; Wu, J.-L.; Chen, Y.; Liu, P.; Zhang, J.; Zhang, S.-Y.; Chen, T.-W.; Zhang, X.-M. Radiomics Model Based on MR Images to Discriminate Pancreatic Ductal Adenocarcinoma and Mass-Forming Chronic Pancreatitis Lesions. Front. Oncol. 2021, 11, 620981.

[24] Qureshi, T.A.; Gaddam, S.; Wachsman, A.M.; Wang, L.; Azab, L.; Asadpour, V.; Chen, W.; Xie, Y.; Wu, B.; Pandol, S.J.; et al. Predicting Pancreatic Ductal Adenocarcinoma Using Artificial Intelligence Analysis of Pre-Diagnostic Computed Tomography Images. Cancer Biomark. 2022, 33, 211–217.

[25] Mohamad Sehmi, M.N., Ahmad Fauzi, M.F., Wan Ahmad, W.S.H.M. and Wan Ling Chan, E., 2022. Pancreatic cancer grading in pathological images using deep learning convolutional neural networks. *F1000Research*, *10*, p.1057.

[26] Upendra, V. and Puviarasi, R., 2022. Pancreatic Cancer Prediction Using Hierarchical Convolutional Neural Network and Visual Geometry Group16 CNN Approach on Accuracy and Specificity Performance Measures. *ECS Transactions*, *107*(1), p.11927.

[27] Khasawneh, H., Patra, A., Rajamohan, N., Suman, G., Klug, J., Majumder, S., Chari, S.T., Korfiatis, P. and Goenka, A.H., 2022. Volumetric Pancreas Segmentation on Computed Tomography: Accuracy and Efficiency of a Convolutional Neural Network Versus Manual Segmentation in 3D Slicer in the Context of Interreader Variability of Expert Radiologists. *Journal of Computer Assisted Tomography*, pp.10-1097.

[28] Chen, X., Wang, W., Jiang, Y. and Qian, X., 2023. A dual-transformation with contrastive learning framework for lymph node metastasis prediction in pancreatic cancer. *Medical Image Analysis*, *85*, p.102753.

[29] Chen, P.T., Wu, T., Wang, P., Chang, D., Liu, K.L., Wu, M.S., Roth, H.R., Lee, P.C., Liao, W.C. and Wang, W., 2023. Pancreatic cancer detection on CT scans with deep learning: a nationwide population-based study. *Radiology*, *306*(1), pp.172-182.

[30] Chegireddy, R.P.R. and Srinagesh, A., 2023. A Novel Method for Human MRI Based Pancreatic Cancer Prediction Using Integration of Harris Hawks Varients & VGG16: A Deep Learning Approach. Informatica, 47(1).

[31] Sarac D, Badza Atanasijevic M, Mitrovic Jovanovic M, Kovac J, Lazic L, Jankovic A, Saponjski DJ, Milosevic S, Stosic K, Masulovic D, Radenkovic D, Papic V, Djuric-Stefanovic A. Applicability of Radiomics for Differentiation of Pancreatic Adenocarcinoma from Healthy Tissue of Pancreas by Using Magnetic Resonance Imaging and Machine Learning. Cancers (Basel). 2025 Mar 27;17(7):1119. doi: 10.3390/cancers17071119. PMID: 40227615; PMCID: PMC11987955.

[32] A. Pravamanjari, S. Swain and P. K. Mallick, "Advanced Detection and Classification of Pancreatic Cancer in CT Images Using Swin Transformer Architecture," *2025 International Conference on Emerging Systems and Intelligent Computing (ESIC)*, Bhubaneswar, India, 2025, pp. 288-293, doi: 10.1109/ESIC64052.2025.10962786.

[33] Viriyasaranon T, Chun JW, Koh YH, Cho JH, Jung MK, Kim SH, Kim HJ, Lee WJ, Choi JH, Woo SM. Annotation-Efficient Deep Learning Model for Pancreatic Cancer Diagnosis and Classification Using CT Images: A Retrospective Diagnostic Study. Cancers (Basel). 2023 Jun 28;15(13):3392. doi: 10.3390/cancers15133392. PMID: 37444502; PMCID: PMC10340780.